Effective breather trapping mechanism for DNA transcription

Julian J.-L. Ting*
Institute für Festkörperforschung, Forschungszentrum Jülich GmbH, Postfach 1913, D-52428 Jülich, Germany

Michel Peyrard†
Laboratoire de Physique de l'Ecole Normale Supérieure de Lyon, CNRS URA 1325, 46 allée d'Italie, 69007 Lyon, France
(Received 5 June 1995; revised manuscript received 31 August 1995)

Collective coordinate and direct numerical integration methods are applied to the analysis of a one-dimensional DNA model. A modification of the coupling constant in an extended region is found to be less selective towards the breather it can trap than an isolated impurity. Therefore it provides a possible physical mechanism for the effect of an enzyme on DNA transcription.

PACS number(s): 87.10.+e, 03.40.Kf

I. INTRODUCTION

The first step of the transcription of deoxyribonucleic acid (DNA) is a local opening of the double helix that extends over about 20 base pairs. Such local unwindings of the helix can be obtained by heating DNA to about 70 °C. But in the life of an organism they must occur at physiological temperature. This is achieved by the action of an enzyme [1]. However, one may wonder how this can be possible since, whatever its origin, the local opening requires the breaking of the same number of hydrogen bonds, hence the same amount of energy, and the enzyme does not bring in energy. However, under normal physiological conditions there are thermal fluctuations along the DNA chain. They can be weakly localized by nonlinear effects to generate what biologists call the "breathing of DNA." But their intensity is not high enough to open the double helix over many base pairs. A possible pathway to the opening would be to collect the thermal energy that is present along the molecule. This could be the role of the enzyme. From a physicist's point of view, the effect of an enzyme can be considered as a perturbation to the DNA lattice.

Recently Forinash *et al.* considered the interaction between a mass impurity on a DNA chain and thermal nonlinear waves described as breathers traveling along the chain [2]. They found that the impurity is selective toward the breather it can trap. Although this is a first indication that a defect can contribute to localizing energy in a nonlinear chain, it does not appear to be a good model for the action of an enzyme because, with such a localized defect, only some predefined frequencies of the thermal fluctuations would contribute to bringing in the energy. Therefore one may ask whether there exists any other mechanism more efficient at trapping energy.

One learns from biological studies that some proteins make contact with DNA at multiple sites [3,4]. Moreover the transcription enzyme actually bends DNA toward itself. It has the effect not only of modifying the mass at some sites but also of modifying the coupling constants along the strands. The bases that are inside the bend are brought closer to each other while the ones that are outside are moved farther apart. Although the variation of the distances between neighboring bases may be rather small, it can have a large effect because the interaction between bases is due to the overlap of π electrons over the whole surface of the planar bases. We examine in this paper whether the interaction of the enzyme with more than one site might be more efficient for trapping breathers than isolated impurities by studying the effect of an extended modification of the coupling along the DNA chain.

The effect of bending and twisting to modify the elasticity of DNA has been considered previously by Barkley and Zimm [5] and by Marko and Siggia [6], but they did not study the consequences of base pair opening. Salerno [7] considered the dynamical properties of a DNA promoter that has some similarities to our problem because we treat here the enzyme as an inhomogeneity due to an external effect while he considered inhomogeneities from the DNA composition itself. However, he was interested in kinks while we study breathing modes. On a more abstract level we are investigating here a nonlinear model, with an "extended defect," and we try to understand the interplay between nonlinearity and disorder. In the harmonic case, a one-dimensional chain with isolated defects has been considered before by Montroll and Potts [8]. However, besides the introduction of nonlinearity, one should also note that for the type of extended defect that we consider, there is no evanescent local mode which would couple to a breather as in the case considered by Forinash *et al.*, so that the mechanism for energy localization must be different.

II. DNA LATTICE MODEL

If one neglects the small longitudinal motion and concentrates on the stretching of the base pairs, DNA can

*Permanent address: Physics Institute, Tsing-hua University, Hsin-Chu, Taiwan 30043, Republic of China.
†Electronic address: mpeyrard@physique.ens-lyon.fr

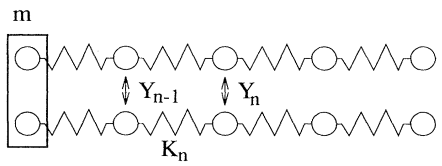

FIG. 1. One-dimensional lattice model of DNA.

be described by a simple one-dimensional model [9] that consists of an array of harmonically coupled particles subjected to a Morse potential. Such a model is sufficient to provide a good qualitative description of the thermal denaturation of the molecule [10]. If one treats a chain with inhomogeneous coupling, the equations of motion read

$$m\frac{\partial^2 Y_n}{\partial T^2} - K_{n+1}(Y_{n+1}-Y_n) + K_n(Y_n - Y_{n-1}) - 2D\alpha e^{-\alpha Y_n}(e^{-\alpha Y_n}-1) = 0 , \quad (1)$$

in which α and D are parameters for the Morse potential [11], which have dimensions of inverse length and energy respectively, and n is the site index. Figure 1 shows the geometry and the coordinate used. It is convenient for the analytical calculations to transform these equations into a dimensionless form by defining the dimensionless variables

$$y_n = \alpha Y_n , \quad (2)$$

$$t = \sqrt{\frac{D\alpha^2}{m}}T , \quad (3)$$

$$k_n = \frac{K_n}{D\alpha^2} . \quad (4)$$

The equations become

$$\frac{\partial^2 y_n}{\partial t^2} - k_{n+1}(y_{n+1}-y_n) + k_n(y_n - y_{n-1}) - 2e^{-y_n}(e^{-y_n}-1) = 0 . \quad (5)$$

One notices that the last set of equations contains only one parameter, the coupling constant. In order to represent the perturbation due to the enzyme, one could imagine the local modification of any of the parameters of Eq. (1), but it is likely that the presence of an enzyme will affect the coupling constant through the bending of the molecule. Moreover, previous studies of the role of disorder on the dynamics of the DNA model [12] have shown that the formation of open regions in the model is much more sensitive to modulations of the coupling constant than to changes in other parameters. Therefore we only consider here an extended perturbation of the coupling constant. An additional possibility for modeling the enzyme specificity is, however, examined in the discussion.

Since we do not know how to solve the discrete case, we transform the set of equations (5) into the corresponding continuous partial differential equation. In the continuum limit, with a Taylor expansion in the potential term, which assumes small amplitude oscillation, Eq. (5) becomes

$$\frac{\partial^2 y}{\partial t^2} - \frac{\partial}{\partial x}\left(k_1\frac{\partial y}{\partial x}\right)d^2 + 2\left(y - \frac{3}{2}y^2 + \frac{7}{6}y^3\right) = 0 , \quad (6)$$

in which d is the lattice spacing and k_1 is a space-dependent coupling constant. We set d equal to unity in the following calculations.

III. THE PERTURBED NONLINEAR SCHRÖDINGER EQUATION

Equation (6) can be transformed into a perturbed nonlinear Schrödinger equation by a multiple-scale expansion [13,14]. Assuming that the amplitude of the thermal oscillation is small $y \approx \epsilon\phi$, we perform the expansion

$$\phi = F_0 + \epsilon F_1 + \epsilon^2 F_2 + O(\epsilon^3) , \quad (7)$$

$$\frac{\partial}{\partial t} = \frac{\partial}{\partial t_0} + \frac{\partial}{\partial t_1}\epsilon + \frac{\partial}{\partial t_2}\epsilon^2 + O(\epsilon^3) , \quad (8)$$

$$\frac{\partial}{\partial x} = \frac{\partial}{\partial x_0} + \frac{\partial}{\partial x_1}\epsilon + \frac{\partial}{\partial x_2}\epsilon^2 + O(\epsilon^3) . \quad (9)$$

Moreover, we assume a modulation of the coupling constant of the order of ϵ, i.e.,

$$\frac{\partial k_1}{\partial x} \approx \frac{\partial k_1}{\partial x_1}\epsilon . \quad (10)$$

Equating like powers of ϵ yields a sequence of equations, in ascending powers of ϵ,

$$\frac{\partial^2 F_0}{\partial t_0^2} - k_0\frac{\partial^2 F_0}{\partial x_0^2} + 2F_0 = 0 , \quad (11)$$

$$\left(\frac{\partial^2 F_1}{\partial t_0^2} + 2\frac{\partial^2 F_0}{\partial t_0 \partial t_1}\right) - \frac{\partial k_1}{\partial x_1}\frac{\partial F_0}{\partial x_0} - k_0\left(\frac{\partial^2 F_1}{\partial x_0^2} + 2\frac{\partial^2 F_0}{\partial x_0 \partial x_1}\right) + 2\left(F_1 - \frac{3}{2}F_0^2\right) = 0 , \quad (12)$$

and higher-order equations, in which k_0 is the unperturbed coupling constant. Solving for equations in each order of ϵ sequentially one obtains

$$F_0 = u(x_1, x_2, t_1, t_2)e^{i(qx_0 - \omega t_0)} + \text{c.c.} , \quad (13)$$

$$F_1 = \frac{3}{2}|u|^2 + \frac{3u^2}{-4\omega^2 + 4k_1 q^2 + 2}e^{2i(qx_0 - \omega t_0)} + \text{c.c.} , \quad (14)$$

and the dispersion relation $\omega^2 = \omega_0^2 + k_0 q^2$, with $\omega_0^2 = 2$. From the vanishing of the secular equation at $q = 0$ one obtains the perturbed nonlinear Schrödinger equation (NLS) at order ϵ^2

$$2i\omega\frac{\partial u}{\partial t_2} + \frac{\partial k_1}{\partial x_1}\frac{\partial u}{\partial x_1} + k_1\frac{\partial^2 u}{\partial x_1^2} + 8u|u|^2 = 0 . \quad (15)$$

We can further rescale the equation into a standard form: Defining the dimensionless variables

$$\hat{k}(\hat{x}) = \frac{k_1}{k_0} - 1 , \quad (16)$$

$$\hat{u} = \sqrt{\frac{8}{\omega^2}}u , \quad (17)$$

$$\hat{x} = \sqrt{\frac{\omega^2}{2k_0}} x_1 , \tag{18}$$

$$\hat{t} = \frac{\omega}{2} t_2 , \tag{19}$$

with $\hat{k}$ being the normalized deviation coupling in the vicinity of the enzyme, one obtains the perturbed dimensionless NLS

$$i\hat{u}_{\hat{t}} + \frac{1}{2}\hat{u}_{\hat{x}\hat{x}} + \hat{u}|\hat{u}|^2 + \frac{1}{2}\frac{\partial}{\partial \hat{x}}(\hat{k}\hat{u}_{\hat{x}}) = 0 \tag{20}$$

and the corresponding Lagrangian density

$$\Lambda = \frac{i}{2}(\hat{u}^*\hat{u}_{\hat{t}} - \hat{u}\hat{u}^*_{\hat{t}}) - \frac{1}{2}(1+\hat{k})|\hat{u}_{\hat{x}}|^2 + \frac{1}{2}|\hat{u}|^4 . \tag{21}$$

In the following section we drop the caret for nomenclature simplicity.

IV. ONE-SOLITON COLLECTIVE COORDINATE ANALYSIS

The collective coordinate method, which is a particle description of the soliton in contrast to the field description given by the Lagrangian, provides a good way to study the influence of a perturbation on a soliton. The spirit is the same as using the center of mass to analyze the behavior of a system of particles.

Without the perturbating term in Eq. (20), one has a breather solution

$$u(x,t) = \eta \mathrm{sech}[\eta(x-u_e t)] e^{iu_e(x-u_c t)} + \text{c.c.} , \tag{22}$$

in which $\eta = \sqrt{(u_e^2 - 2u_e u_c)/(2PQ)}$, where u_e is the envelope velocity, u_c is the carrier velocity, and $P = 1/2$, $Q = 1$ are coefficients of the second space derivative and the nonlinear terms in Eq. (20), respectively. In view of this solution, we use an ansatz for the collective coordinate analysis

$$u(x,t) = \eta \,\mathrm{sech}(\eta x - \zeta)\, e^{i(\phi + \xi x)} , \tag{23}$$

where the parameters η, ζ, ϕ, ξ are functions of t. For an unperturbed system this implies the following relations between the parameters:

$$\eta = \sqrt{u_e^2 - 2u_e u_c} , \tag{24}$$

$$\zeta = u_e \eta t , \tag{25}$$

$$\xi = u_e , \tag{26}$$

$$\phi = -u_e u_c t . \tag{27}$$

At $t = 0$, $\zeta = 0$, and $\phi = 0$ and there are only two parameters left, which is consistent with Eq. (22), because the NLS breather is a two-parameter solution. Even when the breather is far away from the defect, because the ansatz extends to infinity and always experiences the defect, we do not expect these relations to hold for a perturbed system. Hence, in what follows we examine the whole four-parameter space for the equations of motion. Introducing this ansatz into the Lagrangian density Eq. (21) and integrating over space, one obtains an effective Lagrangian

$$L = -2\eta\phi_t - 2\zeta\xi_t + \frac{\eta^3}{3} - \xi^2\eta - \frac{1}{2}\int_{-\infty}^{+\infty} k|u_x|^2 dx \tag{28}$$

and the corresponding Hamiltonian

$$H = -\frac{\eta^3}{3} + \xi^2\eta + \frac{1}{2}\int_{-\infty}^{+\infty} k|u_x|^2 dx , \tag{29}$$

which contains no momentum term.

At this point, we must specify an expression for $k(x)$ to proceed. For algebraic convenience let us choose

$$k = \kappa[\Theta(x+l) - \Theta(x-l)] , \tag{30}$$

in which Θ is the Heaviside step function and l is the half length of the defect. This form of k violates Eq. (10); however, previous works showed that the collective coordinate results are generally robust for the treatment of dynamics in the presence of perturbation [15]; therefore, we can expect to get results that are at least qualitatively correct in spite of this rather crude approximation. Moreover, we shall check them against full numerical simulations in Sec. V.

Introducing the abbreviated notation

$$T_+ = \tanh(\eta l + \zeta) , \tag{31}$$

$$T_- = \tanh(\eta l - \zeta) , \tag{32}$$

$$S_+ = \mathrm{sech}(\eta l + \zeta) , \tag{33}$$

$$S_- = \mathrm{sech}(\eta l - \zeta) , \tag{34}$$

one obtains

$$\int_{-\infty}^{+\infty} k|u_x|^2 dx = \frac{\kappa}{3}(T_+^3 + T_-^3)\eta^3 + \kappa(T_+ + T_-)\xi^2\eta , \tag{35}$$

which characterizes the effect of the defect and decays fast towards zero outside of the impurity region and the equations of motion:

$$\phi_t = \frac{\eta^2}{2} - \frac{\xi^2}{2} - \frac{\kappa}{4}(T_+ + T_-)\xi^2 - \frac{\kappa l}{4}(S_+^2 + S_-^2)\xi^2\eta - \frac{\kappa l}{4}(S_+^2 T_+^2 + S_-^2 T_-^2)\eta^3 - \frac{\kappa}{4}(T_+^3 + T_-^3)\eta^2 , \tag{36}$$

$$\xi_t = -\frac{\kappa}{4}(S_+^2 T_+^2 - S_-^2 T_-^2)\eta^3 - \frac{\kappa}{4}(S_+^2 - S_-^2)\xi^2\eta , \tag{37}$$

$$\zeta_t = \xi\eta + \frac{\kappa}{2}(T_+ + T_-)\xi\eta , \tag{38}$$

$$\eta_t = 0 . \tag{39}$$

As expected, far away from the defect, i.e., when S and T vanish, one recovers the usual relations for the NLS equation because in this case $\xi_t = 0$ so that ξ is a constant that we can denote by u_e. Then $\zeta_t = \xi\eta$ gives $\zeta = u_e\eta t$, as expected, and $\phi_t = (\eta^2 - \xi^2)/2$ gives $\phi = -u_e u_c t$ if u_c is defined by Eq. (24) for η.

In the presence of the defect, the set of nonlinear differential equations for the collective variables cannot be integrated analytically. It is, however, much simpler than the full set of discrete equations since it contains only

three equations. It can be integrated by a fourth-order Runge-Kutta method. One can, however, make general remarks about the properties of the solution before resorting to numerical calculations. The soliton described by the ansatz is an unbreakable entity and moreover the energy given by Eq. (29) is conserved even when a potential well is encountered. Therefore, when the soliton reaches a defect, it may speed up to compensate for the extra energy requirement due to a decrease in coupling energy, as shown in Fig. 2(a), in which a large carrier velocity was chosen to exaggerate the effect. However, the behavior is richer than the one generally found for topological solitons because, in addition to the time-dependent position $\zeta(t)$, the ansatz contains an internal degree of freedom ξ so that the energy can also be transferred between different collective coordinates. With $\kappa < 0$ the last term of Eq. (29) decreases in the region of the defect, therefore ξ^2 has to increase accordingly. If $\kappa > 0$ and the breather is initially inside the defect, it simply slips away as in Fig. 2(b). If it is initially outside, for some suitable range of amplitude it is first slowed down and eventually reflected, as shown in

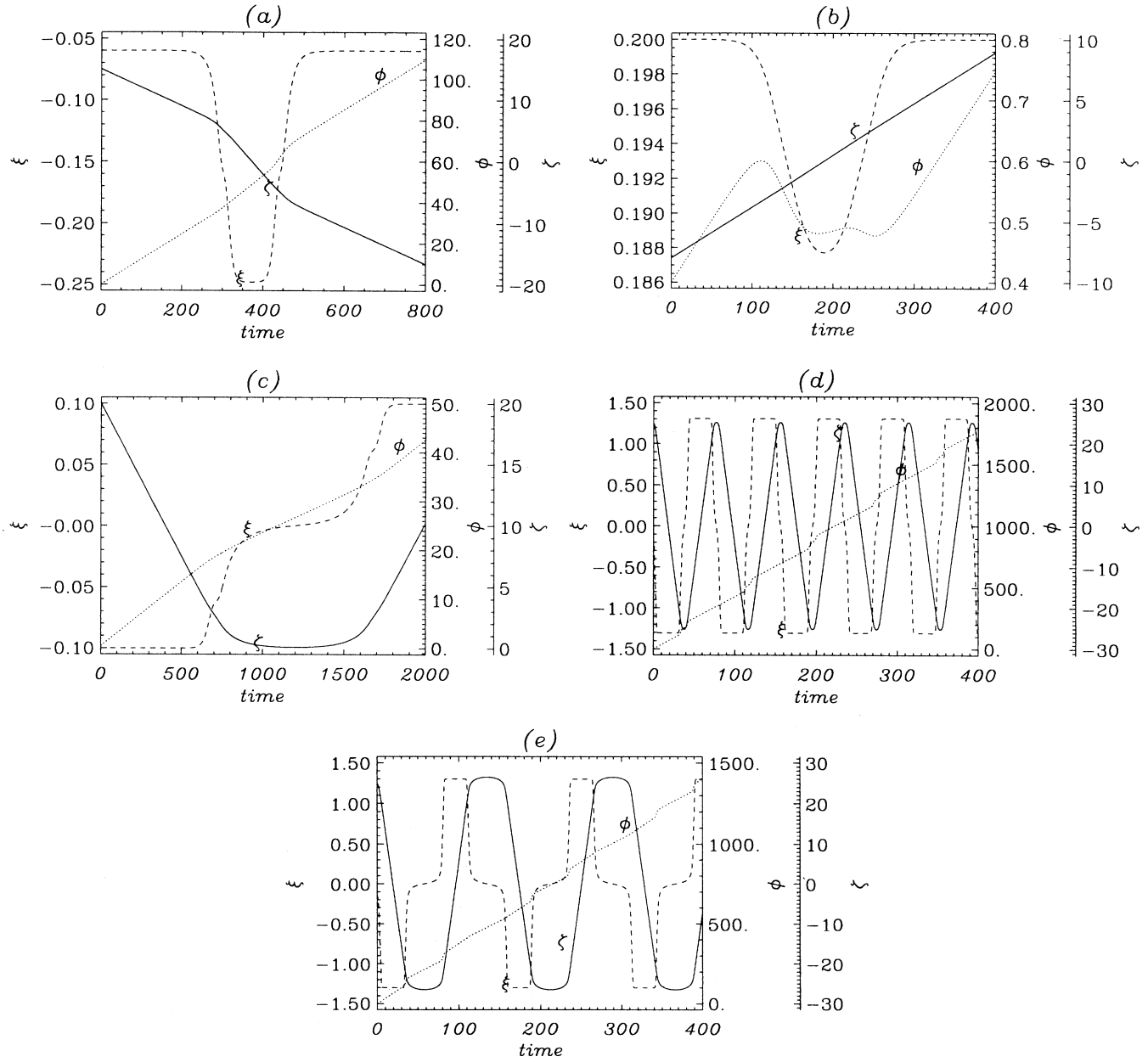

FIG. 2. Evolution of collective coordinates in the presence of a step defect Eq. (30) for $l = 10$: (a) $\eta = 0.5$, $\kappa = -0.4$, $\phi(0) = 0.05$, $\xi(0) = -0.06$, $\zeta(0) = 15$; (b) $\eta = 0.21$, $\kappa = 0.1$, $\phi(0) = 0.4$, $\xi(0) = 0.2$, $\zeta(0) = -8$; (c) $\eta = 0.25$, $\kappa = 0.5$, $\phi(0) = 0.4$, $\xi(0) = -0.1$, $\zeta(0) = 20$; (d) $\eta = 2.3$, $\kappa = -0.5$, $\phi(0) = 0.1$, $\xi(0) = -0.13$, $\zeta(0) = 25$; and (e) $\eta = 2.253$, $\kappa = -0.5$, $\phi(0) = 0.1$, $\xi(0) = -0.13$, $\zeta(0) = 25$.

Fig. 2(c); reflection occurs beyond $\eta \approx 0.25$. For smaller η, breathers pass through the defect, indicating that the broader breathers are less influenced by the presence of defects, just as a large-wheel bike will not be stopped by a pebble or a ditch. In Fig. 2(c) the breather has actually penetrated into the defect before being reflected. When the breather is trapped it oscillates between two positions, which may not be the defect boundary, as shown in Fig. 2(d). For values of η close to the threshold between trapping and nontrapping, the breather slowly turns around at the boundaries as in Fig. 2(e).

A *necessary* condition for a moving breather to be trapped in the above defect is $\kappa < 0$. This statement can be proved through the following argument: a necessary condition for trapping is $\zeta_t = 0$ more than twice, which, according to Eq. (38), is equivalent to

$$\cosh^2 \zeta = 1 - \cosh^2(\eta l) - \kappa \sinh(\eta l) \cosh(\eta l). \quad (40)$$

Since $\cosh^2 > 1$, $k_0 > 0$, and $\eta > 0$, κ has to be less than zero. We have therefore showed that trapping occurs only if the perturbed coupling constant is less than the unperturbed one, which is consistent with our simulations, although it has been proven only in the collective coordinate approach.

Since Eq. (40) contains only ζ, η, κ, and l, if the characters of the defect, i.e., the length l and the strength κ, have been fixed for a given system and the initial position of the breather is chosen, the only factor that characterizes trapping is the breather amplitude. The initial value of ϕ seems to have no consequence on the results. In general, if one finds that a breather passes through a defect for $\kappa < 0$ as in Fig. 2(a), one can obtain trapping by increasing its amplitude.

Because of the helicoidal structure of DNA, a given strand is alternatively inside and outside the bend so that it experiences a periodical modulation of its elasticity by an attached enzyme. We examined the consequence of such a modification by considering the coupling constant modulation

$$k = \kappa[\Theta(x + l) - 2\Theta(x) + \Theta(x - l)] \quad (41)$$

for which the coupling is first increased by κ and then decreased by the same amount if $\kappa > 0$. It can be viewed as a step approximation of one period of a sinusoidal modulation. In general, one finds nothing essentially new with this perturbation because it is only a superposition of two step defects. However, this perturbation is asymmetric in space. By changing the sign of κ we can reverse the orientation of the perturbation with respect to an incoming breather. If $\kappa < 0$, a breather starting from the left side of the defect encounters first the region where the coupling constant is decreased. Table I summarizes the behavior of breathers with various amplitudes and the two possible signs of κ and ξ. For negative κ and positive ξ, the breather is reflected for intermediate η while for large enough η it is trapped. If one switches to positive κ there is still a range of η values that produce reflection, but for large η the breather passes through. If the breather starts from the side where the coupling constant is decreased the trapping can still exist even if the initial position of the breather is far away from the defect, but the pass-through region disappears as expected. These results show that it is the first encounter that determines the trapping. However, for this case of a composite defect the collective coordinate calculation can, in some cases, lead to qualitatively wrong results. The full numerical calculation shown in Fig. 4(a) indicate that the breather can be trapped even if it were coming from the higher side of the defect. This points out the limit of the collective coordinate method for successive perturbations of the breather. The first interaction of the breather with a perturbation appears to be qualitatively well described. But then the perturbed breather is not accurately described by the ansatz. Thus, when it encounters a second perturbation (here the second step in coupling constant), the collective coordinate description fails to describe the interaction.

TABLE I. Behavior of a breather determined by the collective coordinate method with initial values $\phi = -0.4$, $\zeta = -13$ and a two-step defect with length $l = 10$. The table lists the outcome of the interaction of the breather with the defect for different values of η and two different signs for κ.

ξ	Outcome of the interaction	$\kappa = -0.4$	Outcome of the interaction	$\kappa = 0.4$
0.2	passed	< 0.5	passed	< 0.5
	reflected	$0.6 - 1.1$	reflected	$0.6 - 1.4$
	trapped	> 1.2	passed	> 1.5
-0.2	reflected	< 1.1	reflected	all values
	trapped	> 1.2		

V. DIRECT NUMERICAL SIMULATIONS

Since the last example has shown that the collective coordinates cannot provide a full description of the breather dynamics, it is necessary to check them against full numerical simulations of Eqs. (5). Using the breather solution given by Eq. (22) as an initial condition and periodic boundary conditions, we integrate Eqs. (5) with a fourth-order Runge-Kutta scheme and a time step chosen to provide a conservation of energy to an accuracy better than 10^{-6} over a full simulation. The calculations have been tested on different system sizes to make sure that the results are not modified by boundary effects. The ansatz (22) is not an exact solution of the full set of equations because the transformation to the NLS form involved several approximations; however, except for very discrete cases or large amplitude breathers, it provides a rather good solution far away from the defect. As long as the breather is far away from the defect, one generally notices only a small decay of the initial energy peak due to radiation.

Full numerical calculations have the advantage of allowing radiation and breaking of a breather. Furthermore, although the collective coordinate method starts from the perturbed NLS, which requires small u_e and u_c and hence small amplitude, the full numerical calculations do not have this restriction. In what follows we show both the energy distribution and the breather am-

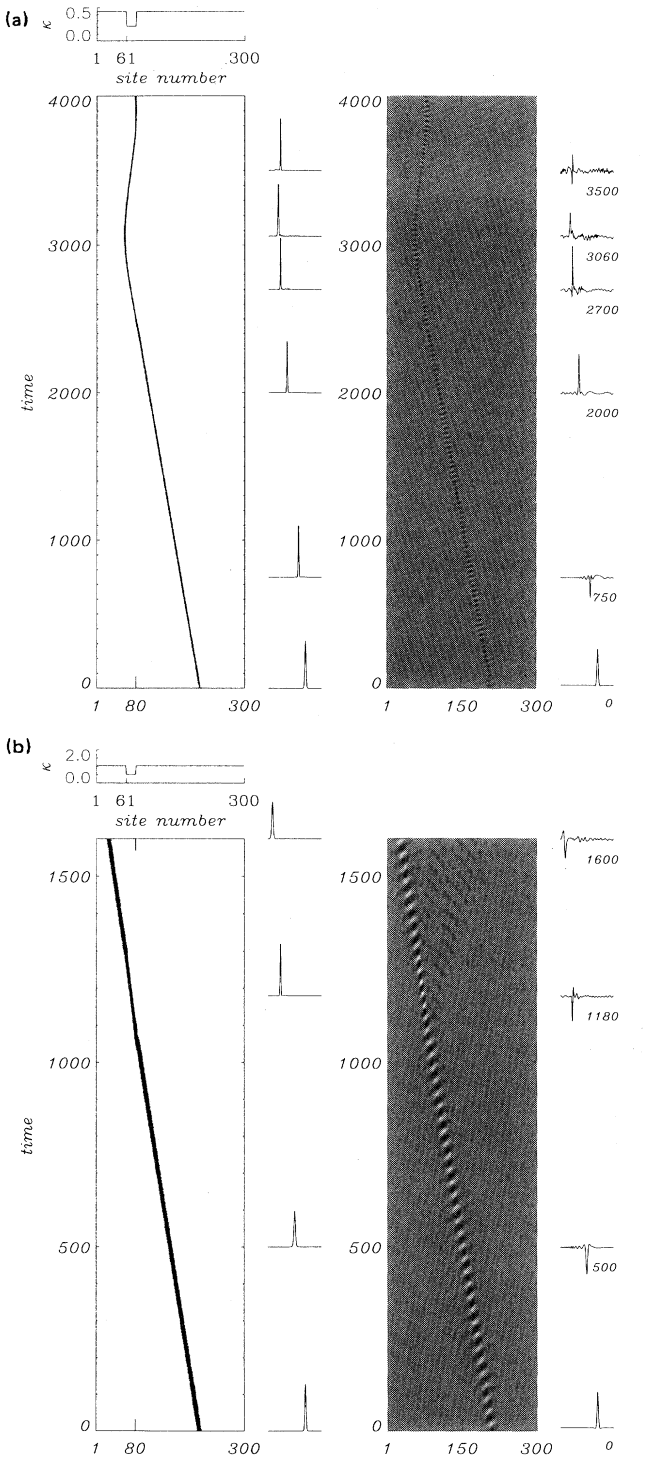

FIG. 3. Halftone plots of the energy distribution of breather evolutions (left) and the corresponding amplitudes (right) from direct numerical integration of Eq. (5). In each figure the top inset shows the variation of the coupling constant used for the calculation, while the right insets show snapshots of the breather energy or amplitude distributions. Defect positions are shown in the plot's axis. (a) $K_n = 0.44$ outside the defect, $K_n = 0.22$ for the defect. $X(0) = 210$, $u_c = 0.13$, $u_e = -0.1$. (b) $K_n = 1.04$ outside the defect, $K_n = 0.52$ for the defect. $X(0) = 210$, $u_c = 0.13$, $u_e = -0.1$.

plitude. The energy distribution is more relevant to the opening of the DNA chain while the breather amplitude allows a comparison with the results of the collective coordinate calculations.

Figure 3(a) is a typical case for trapping at an equivalent amplitude $\eta = 0.19$. The correspondence is made from Eqs. (24) and (26). The threshold for trapping predicted by collective coordinate is higher ($\eta = 1.01$ for a breather initially at $x = 12$ when both systems have the same dimensionless coupling constant). As noticed earlier, it is not surprising to find such a discrepancy because we have used a sharp perturbation that violates the condition (10). However, the full simulations confirm the qualitative predictions of the collective coordinate calculations: small amplitude breathers are transmitted, while larger ones are trapped. Figure 3(b) shows that the energy distribution around the breather gets sharper in the region of the defect. Therefore a negative perturbation, which tends to trap breathers, is also favorable for base-pair openings since it concentrates the energy of the incoming breathers in a narrow domain. This sharpening of the breather shape occurs when the breather is inside the perturbation domain, whether or not it will stay trapped. One can also find, on the contrary, that if a breather meets a positive perturbation, its energy distribution broadens. This behavior is similar to that of a vortex in shallow water: the vortex becomes wider when it is in shallower water and thinner in deeper water [16]. In the amplitude plot of Fig. 3(b), when the breather reaches the boundary of the defect, one can see two small reflected waves. They were not included in the collective coordinate analysis and their presence explains part of the quantitative discrepancy between the analytical approach and the full simulations. Sometimes one can also notice that the breather changes its oscillation frequency after the collision with the defect.

The results of the full numerical simulations show that, although the collective coordinate analysis is able to predict qualitatively the main features, in particular the existence of a threshold for trapping when the breather amplitudes increases, it is quantitatively wrong. The same conclusion had been found for an isolated impurity [2]. There are several reasons for that. First, we do not know an appropriate ansatz for the original equations of motion (1) and we start from a perturbed NLS Lagrangian that is already approximate. Then we use an ansatz that is localized in space and does not allow for the breaking of the breather or the emission of reflected waves. Finally, the calculation assumes a smooth evolution of the coupling constant while we later use a sharp variation to make the analytical calculation possible. In spite of all their weaknesses, the collective coordinate calculations are, however, useful in gaining insight into the behavior of the breather in the presence of the defect or even drawing general conclusions about the kind of defects that can trap energy as explained above.

Another point of interest is the trapping of *several* breathers in the defect region, which could really enhance the energy density locally and cause local openings in DNA. We show in Fig. 4 examples of trapping for two kinds of coupling constant shapes: Fig. 4(a) shows

an example when the breather comes from the higher side of a two-step defect but is trapped. However, unless favorable conditions occur, we seldom find that two breathers can be trapped inside the same perturbation. When the second breather gets trapped it often kicks out the first breather that was trapped before, as shown in Fig. 4(b). In other cases we noticed that when a first breather is trapped in the defect, a second breather that would have been trapped if it were alone is, on the contrary, reflected. Therefore, if one studies only the positions of the breathers during their first interactions with the extended defect, it seems that the defect will never collect more than the energy of one breather. This is in fact not true, but the complete phenomena require a more detailed analysis. It is interesting to study the evolution of the energy in the region of the defect versus time. An example is shown in Fig. 5. In this case the first breather that interacts with the defect has an amplitude $\eta = 0.2$, which is above the trapping threshold and the second one has an amplitude $\eta = 0.1$, below the threshold. As expected, the first breather is trapped and oscillates around the defect. The second one passes through the defect region that contains the first breather. However, if one looks at the energy density on the three-dimensional plot of Fig. 5(a), one can notice a significant increase of energy density after the interaction of the second breather with the defect. The reason is that the second breather is only *partly* transmitted. A large part of its energy is given to the trapped breather, i.e., it stays in the defect region. The same phenomenon occurs again when the second breather collides a second time with the trapped breather. Due to this complex process, the time evolution of the energy inside the defect region [Fig. 5(c)] is a complicated curve, but it is important to notice that it tends to grow and never falls again to a small value, indicating that the multiple collision process does cause a concentration of energy in the defect region. The origin of this localization of energy does not lie in breather trapping but in breather interactions in the presence of a perturbation and therefore it is not included in the collective coordinate description of Sec. IV. The result is reminiscent of a mechanism described recently for energy localization due to discreteness effects in nonlinear lattices [17]. In both cases the collisions of breathers, perturbed either by a defect or by discreteness, cause energy transfers that, on average, favor the large excitation at the expense of the small one. We have checked that the mechanism is not restricted to a particular case. Figure 6 shows another example in which three breathers with the same initial amplitude $\eta = 0.2$ were sent to the defect. Although the details of the process are different, they lead to the same final result: breather interactions in the presence of the defect tend to favor the formation of a large amplitude breather that concentrates a large

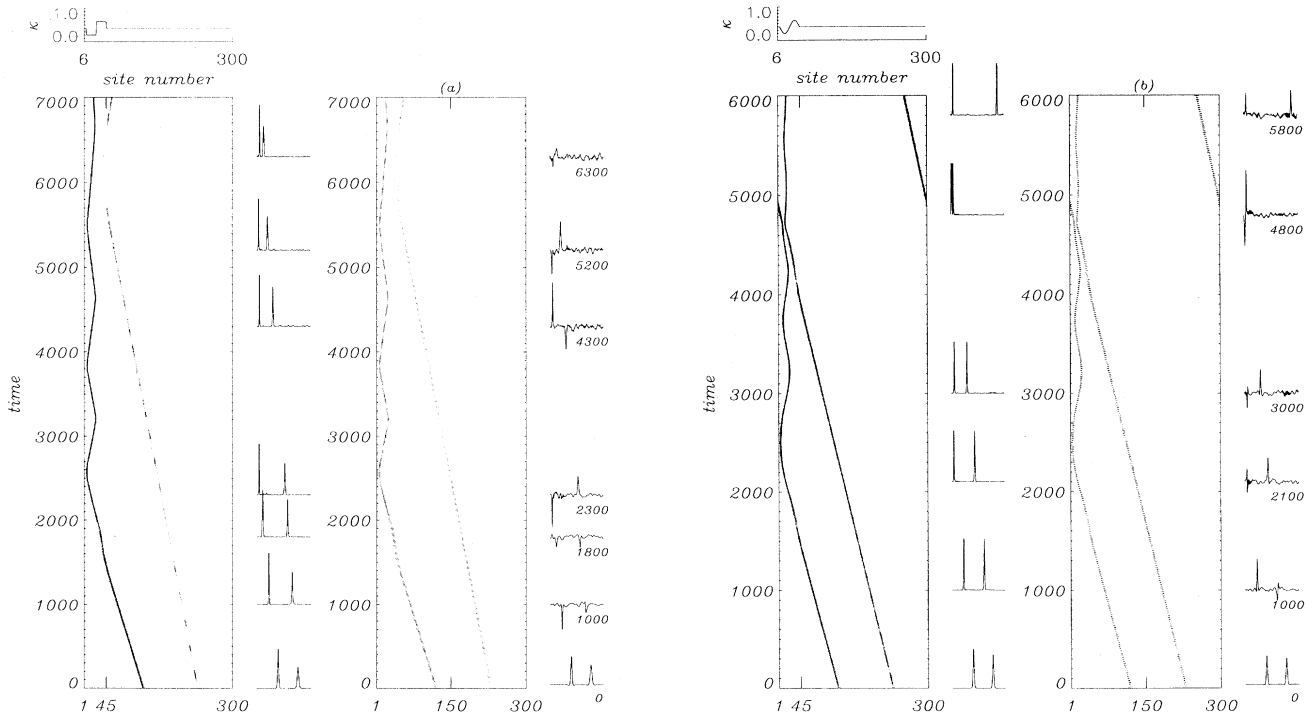

FIG. 4. Halftone plots of the energy distribution of two-breather evolutions (left) and the corresponding amplitudes (right) from direct numerical integration of Eq. (5) and various shapes of defects. In each figure the top inset shows the variation of coupling constant used for the calculation, while the right insets show snapshots of the breather energy or amplitude distributions. The breathers start from $X(0) = 120, 230$. Defect positions are shown in the plot's axis. (a) $K_n = 0.4$ outside the defect, $K_n = 0.2$ inside the defect, and $u_c = 0.13, 0.11$, $u_e = -0.11, -0.07$. (b) $K_n = 0.4$ outside the defect, $K_n = 0.2 \sin(n\pi/l)$ for the defect with n the distance from the center of the defect and l the half length of the defect, and $u_c = 0.13, 0.12$, $u_e = -0.11, -0.1$.

part of the energy of the three incoming breathers and is finally trapped at the defect site. Hence the energy in the defect region settles to a high value. Tests have been performed with various breather amplitudes, leading to the same general result.

VI. CONCLUSION

Using a simple DNA model, we have modeled the effect of a transcription enzyme by an extended modification of the coupling constant along the strands. The results show that such a perturbation is more efficient than an isolated impurity for trapping breathers, in particular because trapping can occur provided that the amplitude of the incoming breather exceeds a threshold instead of requiring breathers with a well defined frequency. This conclusion can be derived from collective coordinate calculations as well as from numerical integration of the full set of equations of motion, although the collective coordinate method overestimates the trapping threshold. One cannot expect quantitative results from the collective coordinate analysis because we have violated at least one basic assumption, Eq. (10), to allow the analytical calculations, but it gives insight into the physics and in particular a necessary condition for breather trapping,

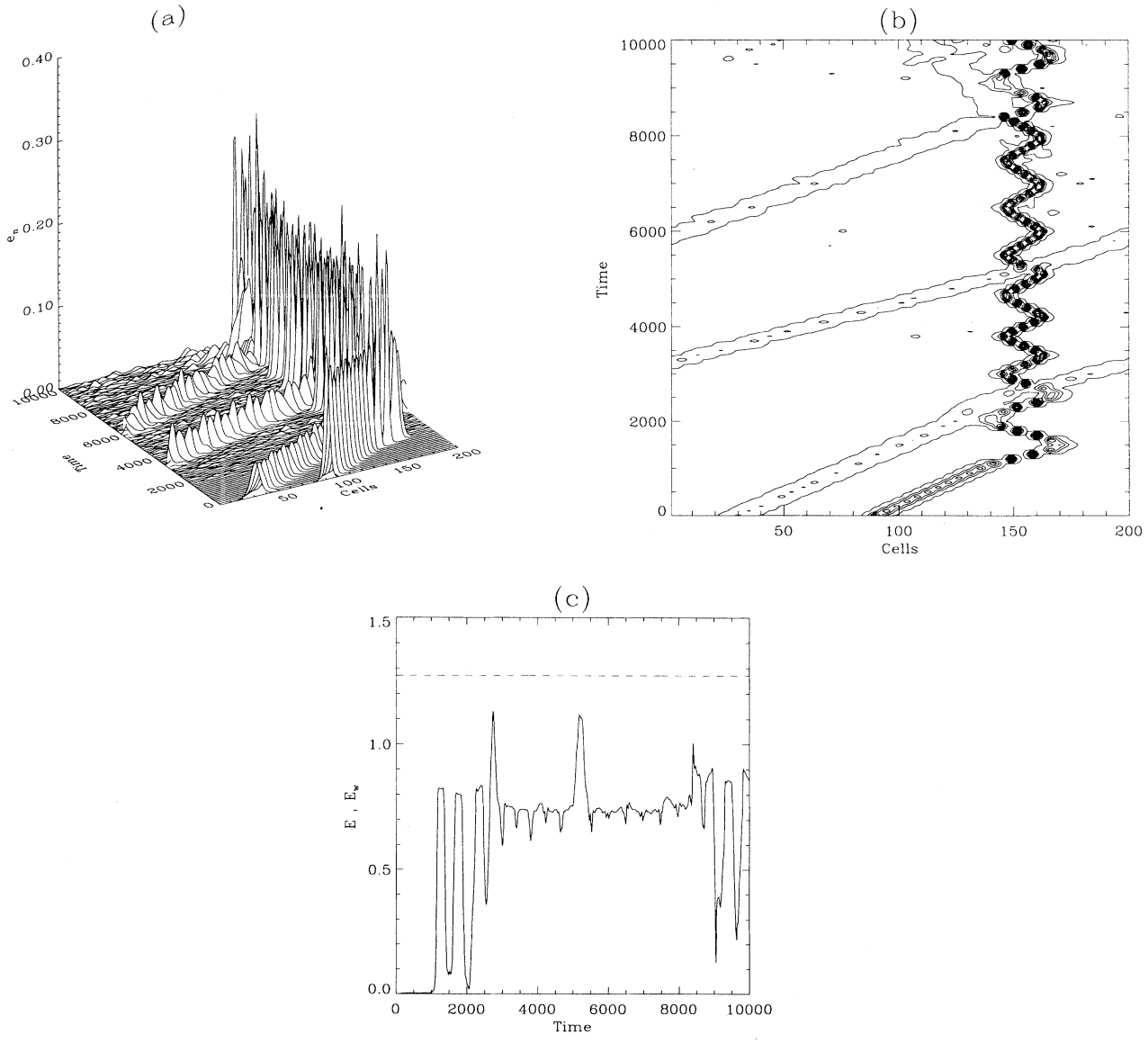

FIG. 5. Interaction of two breathers with an extended defect. $K_n = 1.0$ outside the defect, $K_n = 0.5$ inside the defect, which is 20 cells wide (between cells 145 and 165 in a 200-cell lattice). The parameters of the breathers are $\eta = 0.1$ ($u_e = -0.014, u_c = 0.333$) and $\eta = 0.2$ ($u_e = -0.014, u_c = 1.356$) and both have a carrier wave vector $q = 0.1$. (a) Three-dimensional picture of the energy density e_n versus time and (b) contour plot of the same energy density. (c) Energy E_w inside the defect window (full line) and total energy of the chain E (dotted line) versus time.

which is confirmed by the full simulations. We have also shown that energy exchanges between a first breather, already trapped, and other incoming breathers can lead to a concentration of energy in the region of the defect.

One may wonder whether the results obtained above for specific perturbations are extendable to more realistic cases. Although it is difficult to give general answers to this question, one can gain insight through numerical simulations of the full system. In real DNA one has $D = 0.03$ eV, $\alpha = 4.45$ Å^{-1}, $k_1 = 0.08$ eV/Å^2, $m = 300$ a.m.u. for adenine-thymine base pairs, while for guanine-cytosine pairs we have $D = 0.035$ eV and $k_1 = 0.104$ [10]. This is equivalent to $k_n \approx 0.13$–0.15. In this range of coupling, large amplitude breathers are trapped by discreteness [18]. The collective coordinate calculations suggest that the low amplitude breathers, which can move, will not be trapped by the 20 base-pair defect. Simulations show that it is not necessarily so. For instance, a 20 base-pair defect with $K_n = 0.12$ in a chain with $K_n = 0.15$ can trap breathers of various amplitudes. The energy exchange mechanism in the presence of the defect, discussed above, interferes with discreteness effects that can have a similar influence to localize energy [17]. Therefore, although we have exhibited a mechanism that is active in a wider frequency range than an isolated defect, the calculations performed on a simple model are not sufficient to draw a conclusion about the validity of its use in describing the effect of an enzyme on DNA transcription. It may, however, deserve attention because of its greater efficiency compared to the case of a point defect that was considered previously.

In this work we have modeled the role of the enzyme by modulating only the coupling constant along the strands. As mentioned in the Introduction, other possibilities could be considered, particularly if one attempts to take into account the enzyme specificity, which suggests that the enzyme could have a role other than merely locally bending the molecule. As a first step in this direction, we have considered a local change of the Morse potential in addition to the effect of the bending. Figure 7 shows the result of a numerical simulation where all the conditions are the same as for Fig. 6, except that, in addition to changing the coupling constant inside the defect to model the bending, we have also multiplied the denaturation energy of the base pairs [parameter D of Eq. (1)] by a factor of 0.8. This means that we also assume that the enzyme can have some chemical effect on the reduction of the base-pairing interaction. A comparison of Figs. 7 and 6(b) shows that this modification has a rather drastic effect on the results. It is easy to un-

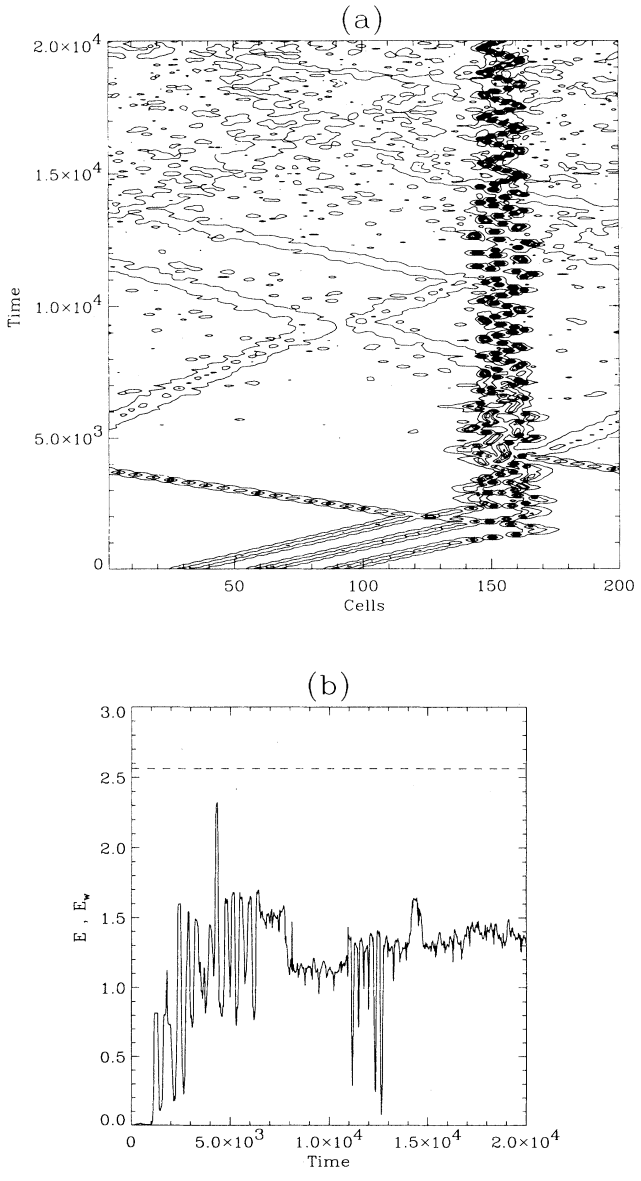

FIG. 6. Interaction of three breathers with an amplitude $\eta = 0.2$ with the same extended defect as in Fig. 5. (a) Contour plot of the energy density in the chain versus time. (b) Energy E_w inside the defect window (full line) and total energy of the chain E (dotted line) versus time.

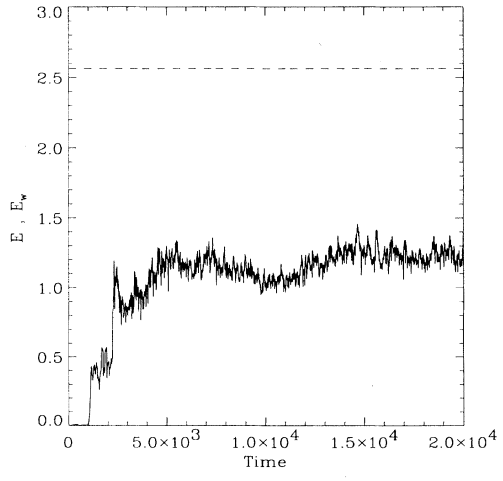

FIG. 7. Energy in the defect region versus time for the interaction of three breathers with an extended defect. The conditions are exactly the same as in Fig. 6, but, in addition to changing locally the coupling constant inside the defect, we also reduce the barrier of the Morse potential by a factor 0.8 in this region to model some enzyme specific action.

derstand qualitatively why, because locally the vibrating frequency of base pairs has been reduced. As we consider low energy breathers, which are the most likely to be excited at physiological temperatures, their frequency, situated below the base-pair linear frequency of the unperturbed region because of the soft nonlinearity of the Morse potential, is, however, very close to the bottom of the phonon band of the unperturbed part of the molecule. As the enzyme lowers the frequencies of the phonon band in the defect region, the breather frequency is now *in resonance* with some modes of the phonon band of the defect. Therefore, when the breather is trapped at the defect site by the bending, it is trapped in a region where it resonates with phonons. As a result, it loses energy by radiation but, as the emitted modes have a frequency below the lowest frequency of the unperturbed lattice, the vibrations are trapped in the defect region. One observes that the trapped breather spreads out its energy inside the defect region. When a second breather comes to this excited defect it is no longer repelled by a highly localized breather as in Fig. 6. Thus it is more likely to penetrate into the defect region too. This makes the energy localization effect more efficient and instead of the large oscillations that were observed in Fig. 6(b), Fig. 7 shows that the energy in the defect region now grows steadily, each new breather having a high probability of adding its contribution. Although it is still preliminary, this example shows that, if one combines the bending effect of the enzyme with some model for its specific action on the promoter site, one can perhaps provide a mechanism with which to achieve the local opening of the double helix, which is required for DNA transcription.

ACKNOWLEDGMENTS

We would like to thank T. Dauxois for helping with computer programming. J.J.-L.T. acknowledges the hospitality of the Laboratoire de Physique de l'Ecole Normale Supérieure de Lyon where part of this work was done. J.J.-L.T. also acknowledges partial support from the National Science Council, Taiwan, Grant No. 84-2911-I-007-030-B21. Part of this work was supported by the EU Science Program through Grant No. SC1*CT91-0705.

[1] C. R. Calladine and H. R. Drew, *Understanding DNA* (Academic, London, 1992).
[2] K. Forinash, M. Peyrard, and B. Malomed, Phys. Rev. E **49**, 3400 (1994).
[3] A. Z. Ansarl, J. E. Bradner, and T. V. O'Halloran, Nature **374**, 371 (1995).
[4] D. A. Erie, G. Yang, H. C. Schultz, and C. Bustamante, Science **266**, 1562 (1994).
[5] M. D. Barkley and B. H. Zimm, J. Chem. Phys. **70**, 2991 (1979).
[6] J. F. Marko and E. D. Siggia, Macromolecules **27**, 981 (1994).
[7] M. Salerno, Phys. Lett. A **167**, 49 (1992).
[8] E. W. Montroll and R. Potts, Phys. Rev. **100**, 525 (1955).
[9] M. Peyrard and A. R. Bishop, Phys. Rev. Lett. **62**, 2755 (1989).
[10] T. Dauxois, M. Peyrard, and A. R. Bishop Phys. Rev. E **47**, 684 (1993).
[11] P. M. Morse, Phys. Rev. **34**, 57 (1929).
[12] M. Peyrard, in *Nonlinearity with Disorder*, Proceedings of the Tashkent Conference, Tashkent, Uzbekistan, 1990, edited by F. Abdullaev, A. R. Bishop, and S. Pnevmatikos (Springer-Verlag, Berlin, 1992).
[13] E. J. Hinch, *Perturbation Methods* (Cambridge University Press, Cambridge, 1991).
[14] M. Remoissenet, Phys. Rev. B **33**, 2386 (1986).
[15] R. Scharf and A. R. Bishop, Phys. Rev. A **43**, 6535 (1993).
[16] D. J. Tritton, *Physical Fluid Dynamics* (Oxford University Press, Oxford, 1988).
[17] T. Dauxois and M. Peyrard, Phys. Rev. Lett. **70**, 3935 (1993).
[18] O. Bang and M. Peyrard, Physica D **81**, 9 (1995).

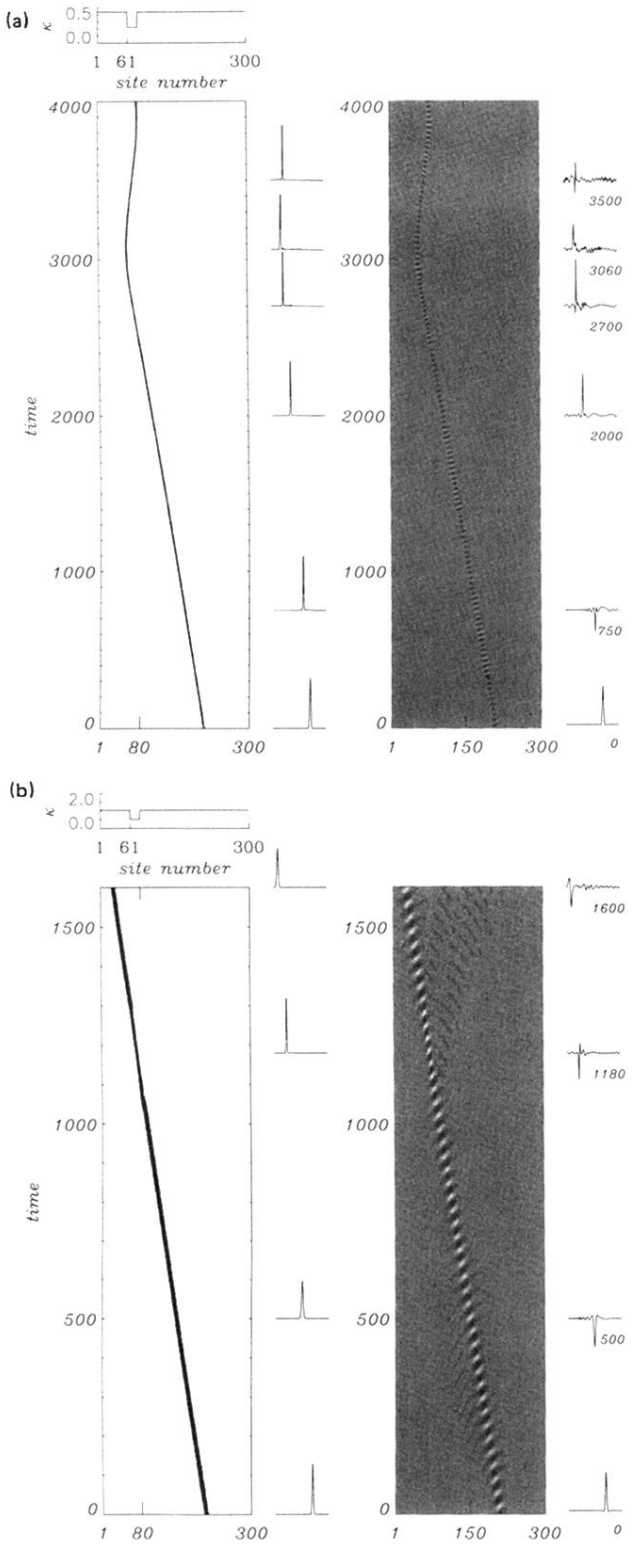

FIG. 3. Halftone plots of the energy distribution of breather evolutions (left) and the corresponding amplitudes (right) from direct numerical integration of Eq. (5). In each figure the top inset shows the variation of the coupling constant used for the calculation, while the right insets show snapshots of the breather energy or amplitude distributions. Defect positions are shown in the plot's axis. (a) $K_n = 0.44$ outside the defect, $K_n = 0.22$ for the defect. $X(0) = 210$, $u_c = 0.13$, $u_e = -0.1$. (b) $K_n = 1.04$ outside the defect, $K_n = 0.52$ for the defect. $X(0) = 210$, $u_c = 0.13$, $u_e = -0.1$.